8. Distribution of Ejecta ❖ ❖ ❖

The overturned rim sequence described in the previous chapter is part of a larger extended blanket of debris. A nearly continuous layer of rubble radiates outward over distances in excess of a kilometer beyond the crater rim. An extensive rotary drilling campaign helped map out the extent of this unit, its thickness, and internal structure (Roddy *et al.*, 1975). Along several transects across the ejecta blanket, debris extends from 1,341 to 1,860 m from crater center, with an average radial distance of 1,543 m (Fig. 8.1). Roddy (1978) estimates the original extent of the continuous ejecta blanket was ~2,500 to 3,000 m.

Previously, mapping by Barringer and Shoemaker (*e.g.*, Fig. 4.4) showed that Coconino debris is prevalent on the south side of the crater and forms patches around the east and north sides of the crater. It is absent on the west side of the crater. Drilling of the ejecta blanket showed further that the thickness of the ejecta blanket is greatest on the south side (see, for example, the lower panel of Fig. 8.1), with some blocks of Kaibab visible in the field at distances of 1.5 km from crater center.

Barringer (1910) argued that a deeper unit of the Coconino (a browner sandstone) is deposited on the southeast side of the crater and, thus, that the deepest units excavated were ejected to the southeast. I do not recall Shoemaker or Roddy reporting a similar distribution, but it is true that some of the Coconino on the southeast side is stained brown.

Roddy *et al*. (1975) examined the contact between the bedded Moenkopi and overlying debris to determine if there was any erosion, brecciation, and mixing when the ejected material landed, similar to the process that generated the Bunte Breccia around the Ries Crater. No significant effects were found. Above normally-bedded Moenkopi, drilling routinely encountered a well-defined overturned sequence of the target lithologies: Moenkopi, Kaibab, Toroweap, and Coconino.

The thickness of the debris, however, is substantially thinner than the pre-impact sequence (*e.g.*, ~20 m on the crater rim versus ~300 m in the walls of transient crater). It is also distributed laterally over greater distances. The existing ejecta blanket beyond the crater rim is 1.6 to 2.6 times wider than the crater radius (from data in Roddy *et al.*, 1975) and distributed over ~7.5 km^2 or ~1,850 acres. In other words, the debris now covers an area ~9 times larger than the crater. This thinning is also apparent in the rotary drill data of Roddy *et al.* (1975), who noted that the Moenkopi becomes thin to discontinuous with increasing distance from the crater. (See Chapter 18 for additional insights about ejecta thinning.) In addition, deeper lithologies (*e.g.*, Coconino) are concentrated on the crater rim, while shallower lithologies (*e.g.*, Moenkopi) occur at greater distances. Thus, the stratigraphy in the pre-impact target is preserved as one walks down slope from the crater rim.

The coarsest material within the ejecta blanket is concentrated near the crater rim. Gilbert (1896), for example, reported blocks of limestone up to 60 ft in diameter (probably Monument Rock) and sandstone up to 100 ft in diameter (the location of which is uncertain) near the crater rim. These are immense blocks of debris and typically scale with the size of the crater-forming event (Fig. 8.2). A carbonate boulder 60 ft in diameter, with a density of 2.24 g/cm^3 (Table 2.3), has an approximate mass of 7.2×10^9 g or over 7,000 metric tons. Monument Rock also sits more than 50 m above its pre-impact position and several tens of meters beyond the crater rim. Barringer (1905) described ejected blocks of debris with masses up to 5,000 tons. These early explorers were particularly impressed with two boulder fields, dominated by Kaibab blocks, that were distributed roughly symmetrically, occurring on both the east and west sides of the crater (Fig. 8.3). As discussed further in Chapter 10, Barringer used these boulder fields in his assessment of the impacting projectile's trajectory.

Although we often idealize the continuous ejecta blanket as a well-ordered set of inverted target strata, local complexities exist within the debris blanket. For example, along the north rim of the crater, the surface of Kaibab ejecta was undulating or hummocky, forming a depression that was filled with Coconino debris (Fig. 8.4). This particular deposit was described by Barringer (1910) as one of the "spurts or jets" of sandstone that surround the crater, thinking they were akin to crater rays. The ejected strata have also been fragmented, so that the overturned units are better described as partially-disrupted, semi-coherent sheets. The degree of disruption increases towards the surface of the ejecta blanket. Overturned Moenkopi is very coherent, Kaibab less so, and Coconino sandstone on top of the debris blanket has been fractured much more severely (Fig. 8.5). A nearly 20 metric ton sample of overturned Coconino demonstrated that fragments had been reduced to 40 × 40 × 90 cm and smaller (Walters, 1966), far smaller than many of the Kaibab boulders in the underling layer of ejected debris. The additional disruption may reflect the inherent structural integrity of the pre-impact lithologies. It may, however, also be a function of the material's position in the overturned sequence. Moenkopi and Kaibab were contained within additional debris, whereas the ejected and overturned Coconino represented an unbounded free surface.

Not surprisingly, the density of material incorporated into the ejecta blanket is less than that of the original target rocks. In a NASA-sponsored study during the Apollo era, 19,320 kg or 10.31 m^3 of ejecta were excavated at the surface to a depth of 2 m. The ejecta was excavated on the overturned flap of the southern rim of the crater, where it is dominated by loose sand and platy blocks of Coconino-Toroweap sandstone. The bulk density of the ejecta was 1.87 g/cm^3 (Walters, 1966), which is 6 to 10% lower than that (1.98 to 2.08 g/cm^3; Table 2.1) of isolated Coconino sandstone fragments that have been used for shock experiments (Ahrens and Gregson, 1964; Shipman *et al.*, 1971; Ai and Ahrens, 2004). A decrease in density is a general property of impacts into consolidated lithologies like those at Barringer Crater. It may not apply, however, to unconsolidated sediments. Following a nuclear test explosion in alluvium (Sedan at the Nevada Test Site), an ejecta density identical to pre-shot target density (1.5 g/cm^3) was measured (Carlson and Roberts, 1963). In some cases, shock may even compress and cement unconsolidated target materials, effectively increasing density in both crater walls and ejecta.

The continuous ejecta blanket represents the bulk of excavated debris, but there are other ejecta components. Isolated blocks of debris were flung far beyond the continuous ejecta blanket. These are sometimes called missile debris and, around experimental explosion craters, have produced secondary craters. Barringer (1910) reported fragments of Kaibab that were ejected 2½ to 3 miles (4 to 5 km) in blocks weighing 50 to several hundred pounds (Table 8.1). In addition, Gilbert (1896) found at least one Kaibab block 3½ miles beyond the crater rim. Rocks landing 3, 4, and 5 km beyond the crater rim were hitting at speeds of about 650 to 850 km/hr, which is about half the sound speed in air (1224 km/hr) and about an order of magnitude less than seismic velocities in the sedimentary rocks around the crater. As far as I know, no secondary craters associated with those blocks have been described. Smaller pebble- to cobble-size components also blanket the surrounding landscape (Figs. 8.6 and 8.7), a feature not evident in any geologic map of the crater.

Also not reliably mapped are denser patches of discontinuous Kaibab ejecta deposits. Grant and Schultz (1993) briefly pointed to a candidate deposit in one of their figures (their Fig. 12). More detailed mapping of that and other nearby deposits (Kring *et al.,* 2015) confirmed they are discontinuous lobes of Kaibab ejecta that landed with horizontal velocities of ~250 to 300 km/s and then skated or flowed radially outward, in one case flowing up a ridge of Moenkopi (Fig. 8.8). Similar patches of Moenkopi might also exist, but they would be difficult to recognize on top of the bedrock Moenkopi or the shale-rich soil that often sits on top of Moenkopi bedrock.

The transition from continuous to discontinuous ejecta around the crater is an issue needing more attention and a mapping project is underway to clarify that distribution (Kring *et al.,* 2015; Durda and Kring, 2015; Schmieder *et al.*, 2017). Shoemaker mapped the surface geology, producing map views of the continuous ejecta. Later, Roddy conducted a drilling campaign to determine a subsurface measure of the continuous ejecta and proposed a more extensive unit (Fig. 8.9). The region between those two limits is currently being remapped (*e.g.*, Schmieder *et al*., 2017) and is revealing additional surficial deposits of Kaibab ejecta and other interesting deposits. For example, a knoll in the southeast quadrant contains both Kaibab and Moenkopi ejecta. The Kaibab is concentrated on the face towards the crater, while Moenkopi debris is concentrated on the far side of the knoll. Thus, as in Fig. 8.8, a lobe of Kaibab debris mantles the crater-facing side of a knoll.

The material in the ejecta curtain that fell to produce the continuous ejecta blanket was traveling on ballistic trajectories. The time required for that material to be emplaced increased with radial distance. Material near the rim landing within a few seconds at relatively low speeds, while material at the edge of the continuous ejecta blanket had times of flight several tens of seconds and would land with speeds in excess of a 100 km/hr (Fig. 8.10),.

There were probably two other debris components beyond the rim of the crater: a fall-out or fallback unit and a base-surge unit. Neither of these units was mapped by Shoemaker, but they are inferred from observations within Barringer Crater and around experimental (particularly nuclear) explosion craters. A fallback debris deposit on top of the overturned ejecta blanket is inferred from fallback debris that is observed within the crater (Chapter 4). It is likely to have covered the crater rim, but its radial extent is unknown. Did it, for example, cover all the overturned ejecta blanket? Or could it have extended even farther? An important component of the fallback unit within the crater walls is meteoritic material and may have also been an important component of the fallback unit beyond the crater rim. Barringer (1910) reported fragments of meteoritic material out to distances of ~5½ mi (Chapter 9). Gilbert (1896) reported a meteoritic mass 8 mi (nearly 12.8 km) east of the crater, which is more than twice the distance of the farthest Kaibab block he observed. In addition, Nininger (1956) reported impact-melted spherules of projectile material out to a distance of 5 mi (8 km) from the crater rim, although erosional transport may have modified their distribution.

Impact melt fragments are another component of fallback debris (Fig. 8.11). Unfortunately, a good survey of its distribution has not been published. Nininger (1956) reported that melt fragments were abundant within 1,500 ft (~0.46 km) of the crater rim, but decreased rapidly at greater radii to a maximum exent of 1½ miles (2.4 km). Taken at face value, this suggests the impact melt in a fallback debris unit extended to greater radii than the continuous overturned ejecta blanket. This is consistent with observations around the Sedan nuclear test explosion in alluvium, which distributed fused material beyond the continuous overturned ejecta blanket, but not as far as some missile ejecta. Unfortunately, erosional transport may have modified the distribution of melt fragments around Barringer Crater, so it is difficult to make an independent assessment of the distribution.

While Shoemaker did not map a fallback unit beyond the crater rim, it is clear that his alluvium deposits were composed of fallback debris. Indeed, recent studies suggest that some of those alluvium deposits may be primary fallback debris deposits, not just reworked, secondary deposits of debris (Kring *et al.*, 2012; see also Chapter 18). Those deposits can be up to (and possibly greater than) 7 m thick.

A base-surge deposit likely formed on top of the fallback unit. A base-surge unit is produced from a collapsing column of the finest components in up-thrown ejecta. It has been observed around several experimental nuclear explosion craters. Unfortunately, no remnant of this unit survives at Barringer Crater, so we can only crudely estimate its distribution. In the case of the Sedan nuclear explosion crater

in alluvium, isolated blocks of debris (missiles) landed up to 3 times farther than the continuous ejecta blanket and the base surge deposit extended more than 5 times farther than the continuous ejecta blanket (Carlson and Roberts, 1963). Thus, using Roddy's measurements of the existing continuous ejecta blanket around Barringer Crater, a base-surge deposit may have radiated outward for distances of 7.5 to 15 km (and possibly farther). Fine-grained base surge deposits are susceptible to wind and can be redistributed within days of crater formation. This unit was probably stripped from the region around the crater very quickly.

Estimates of the total mass of ejected material have varied. Barringer (1910) estimated more than 300 million tons of rock was ejected from the crater. A modern value derived by Roddy *et al.* (1975) is 175 million metric tons, which includes 60, 113.8, and 1.2 million metric tons from the Coconino-Toroweap, Kaibab, and Moenkopi, respectively. Not all of this mass, however, can be accounted for in existing debris deposits. They estimate 100 million metric tons survive in the overturned rim sequence and continuous ejecta blanket; 22.2 million metric tons were redeposited inside the crater; and 5.6 million metric tons were deposited as fallback ejecta. Thus, 27% of the ejected mass is missing. These mass estimates utilized a volume bulking factor of 5% in ejected units, which is based on geophysical estimates of 2.30 g/ cm^3 for an average density of undisturbed bedrock and 2.18 g/cm^3 for the density of the breccia lens. This may be a slightly low correction, given that analyses of the ejected material suggest a 6 to 10% density decrease (1.87 *vs.* 1.98 to 2.08 g/cm^3) measured on the south crater rim (above). Roddy *et al*. (1975) also suggested that the missing mass can be accounted for as (a) material ejected beyond the continuous ejecta blanket, (b) material distributed in fine particles that were lofted high by the impact and carried away by wind, and (c) erosion that has stripped material from the ejecta blanket. They estimate that (a) and (b) explain 5 to 10% of the mass deficit and that the remainder is an erosional loss.

Shoemaker and Kieffer (1974) measured 40 ft (12 m) of erosion on the northeast crater flank. They argue that this is a minimum number and estimate that total rim erosion is 50 to 75 ft (15 to 20 m). They also suggest that erosion may be as much as 100 ft (30 m), assuming Coconino debris was deposited and subsequently eroded where Kaibab ejecta is currently exposed. This result also implies that the outer flank of the crater rim was originally steeper than now observed, because the alluvium and colluvium that covers the Coconino sandstone ejecta pediment softened the slope. It is worth noting that erosion has been more severe in some areas around the crater than in others. Barringer (1910) reported that the silica pits on the southwest side of the crater were a natural arroyo when he arrived, having an expanse of 200 to 300 yds and a depth of 10 to 12 feet. Thus, some sections of the ejecta blanket were severely dissected before any mining operations disturbed them.

While analyzing samples to determine the age of the impact event, Nishiizumi *et al*. (1991) also measured the exposure ages at different levels along an ~10 m-tall Kaibab boulder (Whale Rock; Fig. 8.3 and 18.16) on the west side of the crater. Their analyses suggest the uppermost 8 m of the boulder were uncovered in ~27,000 yrs at an average rate of 30 cm/1000 yrs, and 1.2 m were uncovered in the last 23,000 yrs at an average rate of 5 cm/1000 yrs. Thus, at least where Whale Rock is located, 9 m of finer-grained ejecta has apparently been eroded.

In contrast, Grant and Schultz (1993) reported smaller amounts of erosion around the crater, although they focused their studies on debris farther from the rim crest and on shallower slopes. They based their estimate on the production of coarse erosional lag deposits and the sediment budgets of multiple drainage systems on the flank of the crater. They estimated <1 m of erosion beyond 1/4-1/2 crater radii from the crater rim, although loss of 2 to 3 m of material occurred in small areas. These estimates of erosion are smaller than those in previous studies, but Grant and Schultz (1993) suggest that there are true variations with radial distance from the crater rim: Higher erosional rates determined by

Shoemaker and Kieffer (1974), Roddy *et al.* (1975), and Nishiizumi *et al.* (1991) reflect erosional conditions on or near the steep rim crest, whereas their results reflect erosional conditions on the shallower flanks of the ejecta blanket.

Sitting on, and emerging from, the eroding ejecta blanket are boulders ejected from the crater. An assessment of their size distribution is underway (Durda and Kring, 2015). The work began in the northeast quadrant, where all boulders with diameters >25 cm are being mapped. Thus far, 40,955 boulders have been recorded in that quadrant. Although that is a preliminary study, it is already clear that clusters and rays of boulders were deposited in that quadrant of the crater. Because the type of ejecta varies significantly in different directions around the crater, a proposal to map the boulders in all quadrants has been submitted. Once complete, it will be possible to evaluate how pre-impact target properties (*e.g.*, lithology, stratigraphic thickness, joint spacing) affect the size distribution of ejected boulders. That will, in turn, provide a baseline for assessing ejected boulder size distributions around craters on the Moon and Mars.

A feature of the ejecta blanket often overlooked is its hummocky topography (Fig. 8.12). That topography is unlikely to be a product of post-impact erosion, in part because it would require a circumferential erosion pattern, rather than a downslope-directed and/or radial erosional pattern. The hummocky topography appears to be a primary feature of ejecta emplacement. Part of the hummocky nature of the ejecta blanket may reflect the inverted topography of the pre-impact Moenkopi landscape. However, another important cause of the hummocky topography appears to be shearing of Kaibab away from the crater rim during the emplacement of the ejecta blanket, which was, in some places, further accentuated by normal faults that separated the unit into more discrete blocks (Kring *et al.*, 2011a,b). Evidence for that type of shear and extension of the ejecta blanket is seen along the Crater Rim West trail (Chapter 18).

That shear of Kaibab away from the crater rim is also likely responsible for the surviving distribution of Coconino ejecta around the crater. As can be seen in Shoemaker's geologic map (Fig. 4.4), Coconino ejecta is concentrated on the south side of the crater. Excavated sandstone initially covered the entire ejecta blanket, but most of it has been eroded from the north, west, and east sides of the crater, exposing Kaibab. On the south rim of the crater, however, the base of the overturned Coconino and Toroweap sandstone was lower than anywhere else around the crater, because Kaibab was sheared from the rim sequence. In addition, the dips of the uplifted (and underlying) target units are subdued in the south crater wall. In the measured section, dips are only 15 to 20°, whereas they are typically twice those values elsewhere around the crater. Thus, fault-modification of the normal ejecta process created lower topography and shallower slopes on the south side of the crater, which reduced erosion rates and allowed the Coconino ejecta to survive there.

Table 8.1. Radial extent of impact components

Ejecta Component	Distance from Crater Rim (km)	(crater radii)	Distance from Crater Center (km)	(crater radii)	References
Continuous Overturned Ejecta Blanket					
Observed Range	0.748-1.267	1.46-2.48	1.341-1.860	2.62-3.64	1
Average of Observed Range	0.95	1.86	1.543	3.02	1
Estimate of Average Pre-erosional Extent	1.9-2.4	3.7-4.7	2.5-3.0	4.89-5.87	2
Isolated Blocks of Kaibab					
Observed Maximum	5.6	11	6.2	12	3
Impact Melt Fragments					
Observed Maximum	2.4	4.7	3.0	5.9	4
Meteoritic Fragments of Asteroid					
Observed Maximum	8.8	12	9.3	12	5
	13	25	13.5	26	3
Melted Meteoritic Spherules					
Observed Maximum	8.0-9.6	16-19	8.6-10	17-20	4,6

(1) Roddy *et al.*, 1975; (2) Roddy, 1978; (3) Gilbert, 1896; (4) Nininger, 1956; (5) Barringer, 1910; (6) Rinehart, 1958
Value for crater radii is based on a 1,022 m estimate of a pre-erosional crater diameter measured at the pre-impact elevation (Roddy, 1978). The current average crater rim diameter is taken to be 1,186 m (Roddy, 1978).
I emphasize that the values above are observed distances. Erosion may have affected the distribution of ejecta components.

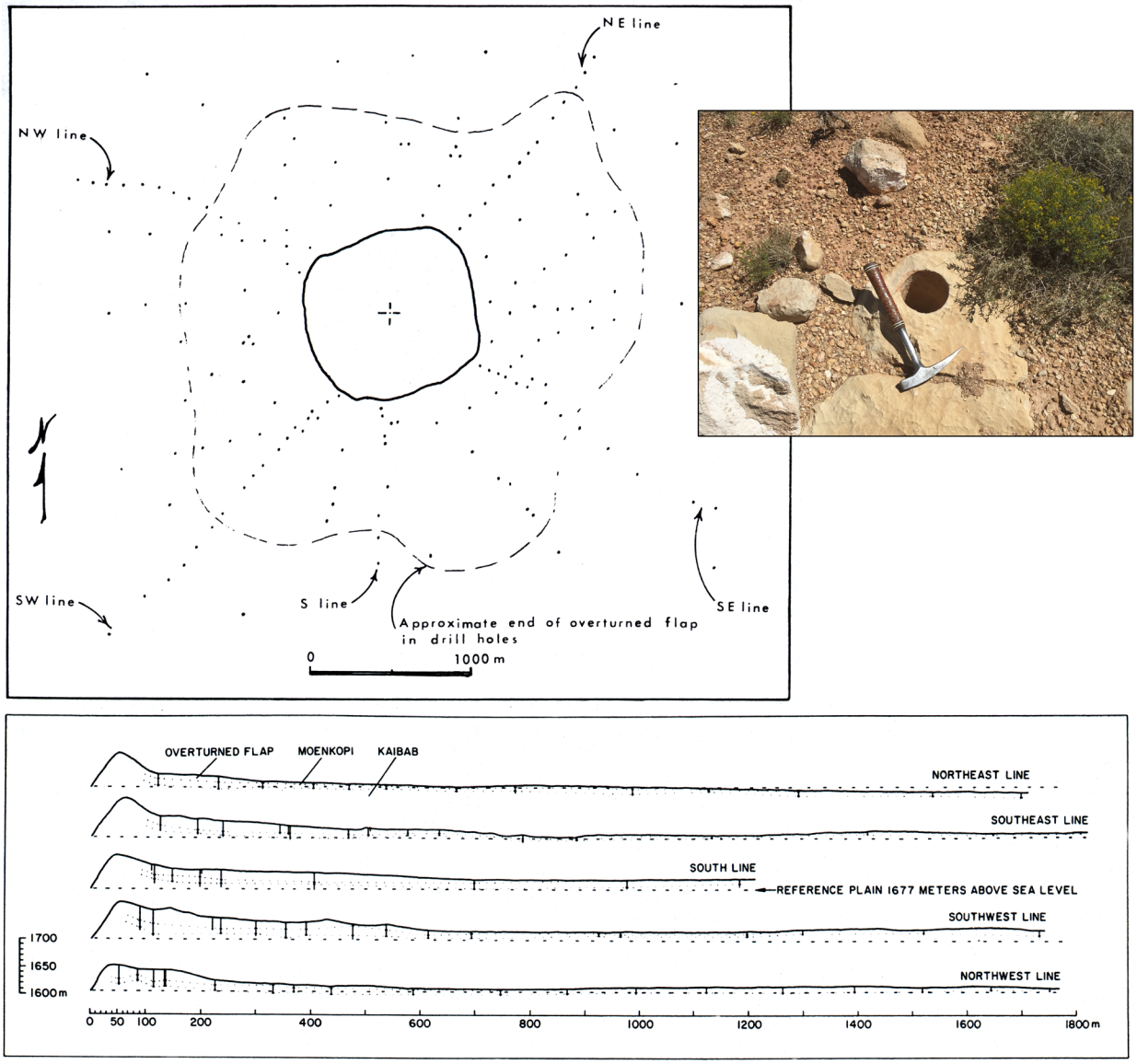

Fig. 8.1. Locations of rotary drill holes around Meteor Crater (top left panel) and generalized geologic cross-sections along five transects (bottom panel). Both panels are from Roddy *et al.* (1975). The lateral extent of the ejecta blanket is mapped in the plan view and illustrates slight asymmetry. The average radial extent of the ejecta blanket around the crater is 1,543 m from crater center. In the cross-sections, the locations of the drill holes are indicated by vertical lines. Subtle dotted lines within each profile also indicate the top and bottom of Moenkopi encountered in the drill holes. These symbols are poorly expressed in the original figure and have not (yet) been redrawn. An example of one of the drill holes is shown in the top right panel with a 33-cm-long hammer for scale.

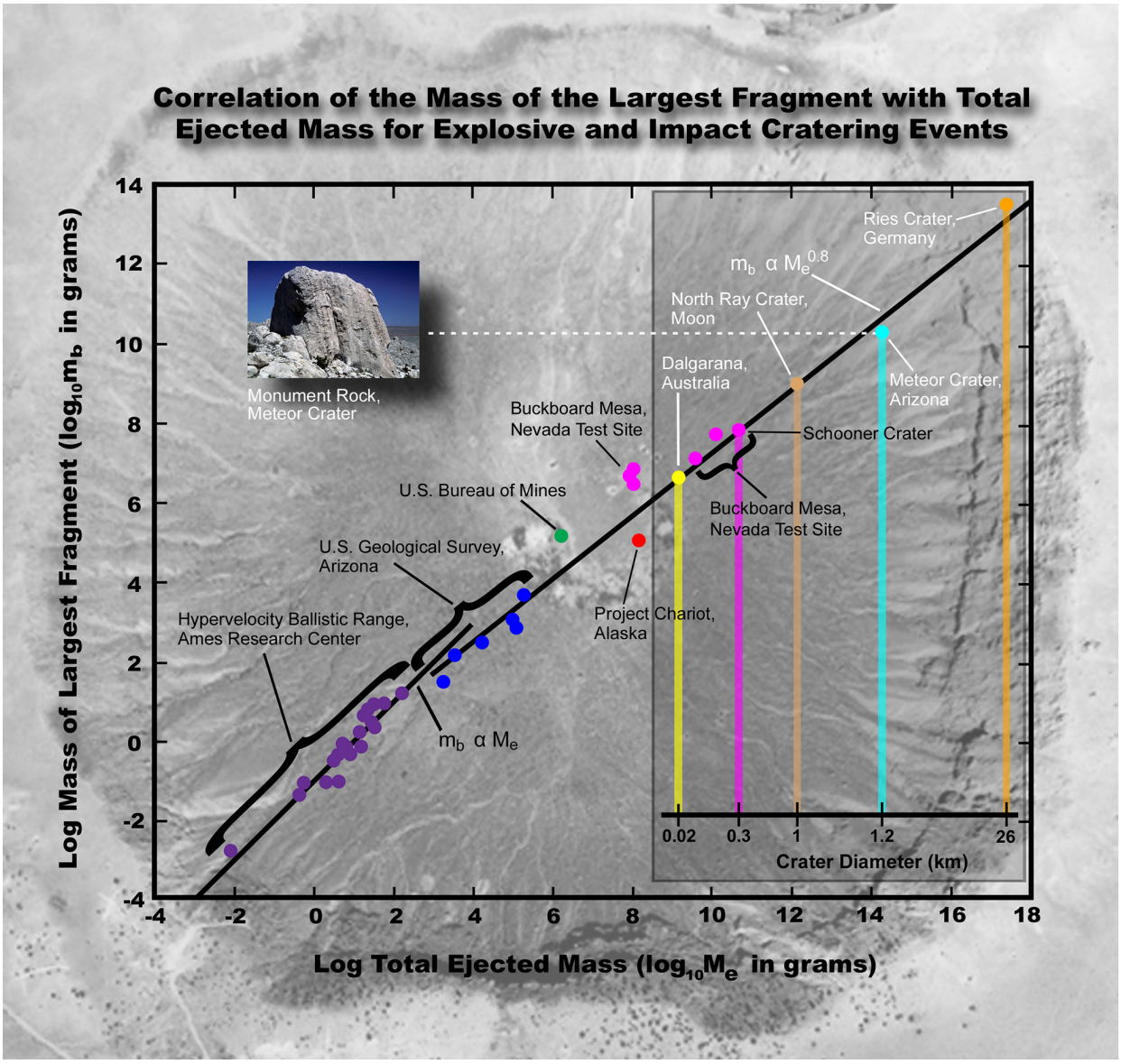

Fig. 8.2. Data from multiple explosion cratering experiments (black labels) and four impact craters (white labels) indicate that the mass of the largest ejected block (m_b) scales with the total mass of ejected material (M_e). The inset illustrates that the mass of the largest ejected block also scales with crater diameter. Blocks of rock ejected from the 1.25 km diameter Meteor Crater approach the size of a garage, while those ejected from the 26 km diameter Ries Crater are the sizes of hills. This diagram is modified from a figure produced by Gault *et al*. (1963). The diagram also includes data from the North Ray Crater on the Moon (Apollo 16 Preliminary Science Report, NASA SP-315, 1972). Image Credit: Andrew Shaner & David A. Kring; and can be downloaded from the LPI Classroom Illustration library at http://www.lpi.usra.edu/exploration/training/resources/

Fig. 8.3. One of two boulder-rich fields within the continuous overturned ejecta blanket. This deposit of boulders is exposed on the west side of the crater, south of Barringer Point. The boulder field contains Whale Rock, which was originally buried within the ejecta blanket. Erosion of finer-grained and more friable ejecta components has exposed the boulders. The inset shows the same boulder field from a southeast-looking vantage point with a slightly different illumination angle. The surface of the surviving ejecta blanket is much steeper on the rim crest than it is at greater radii from crater center.

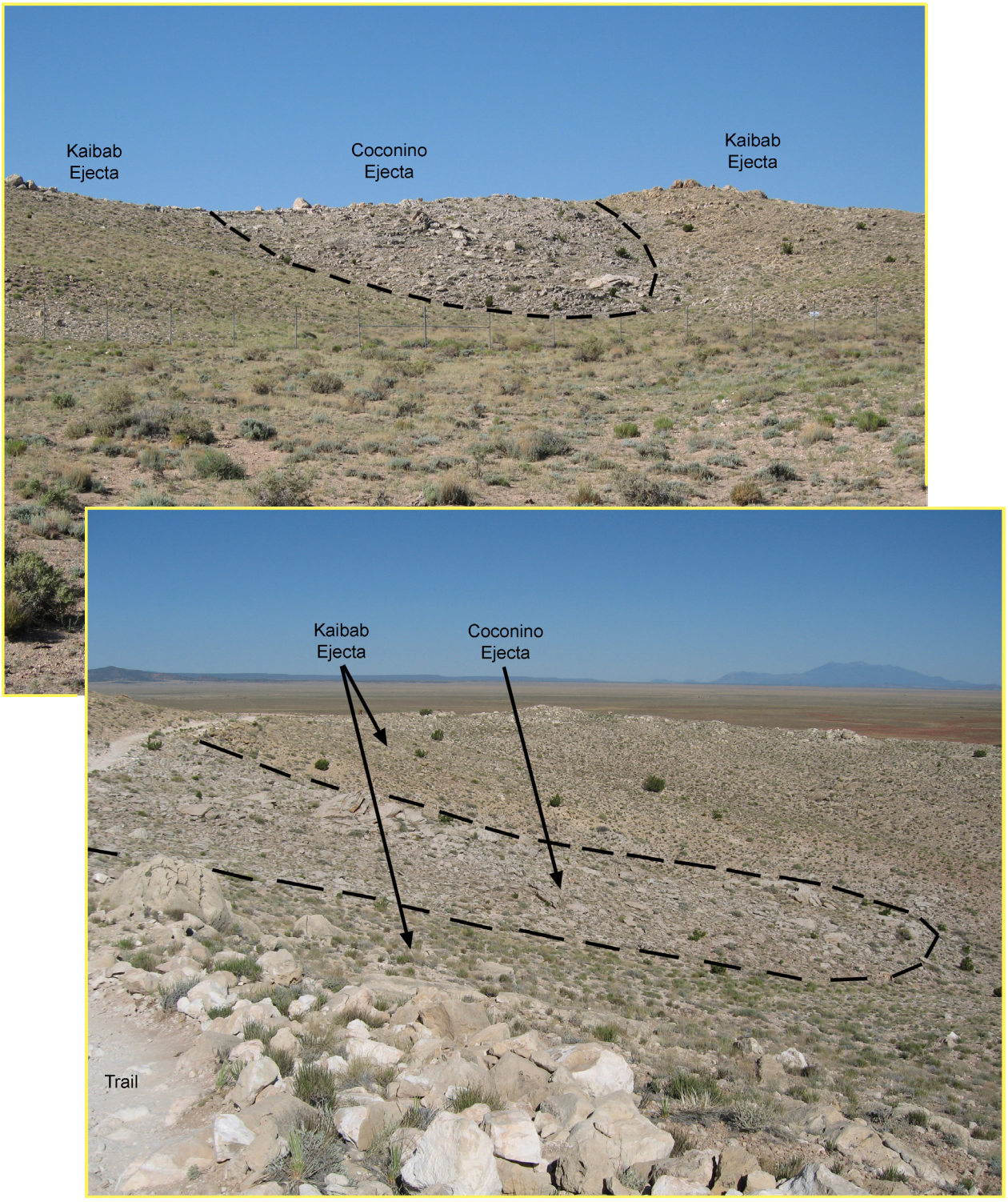

Fig. 8.4. The surface of ejected Kaibab debris was irregular, forming a depression in this location (top panel) that was filled with a wedge of Coconino sandstone debris (top and bottom panels). The deposit is on the north side of the crater. The view of the top panel (looking south) is from the road that leads up to the museum complex. The view in the bottom panel (looking northwest) is from the trail along the north rim, between the current museum complex and remnants of an old museum building.

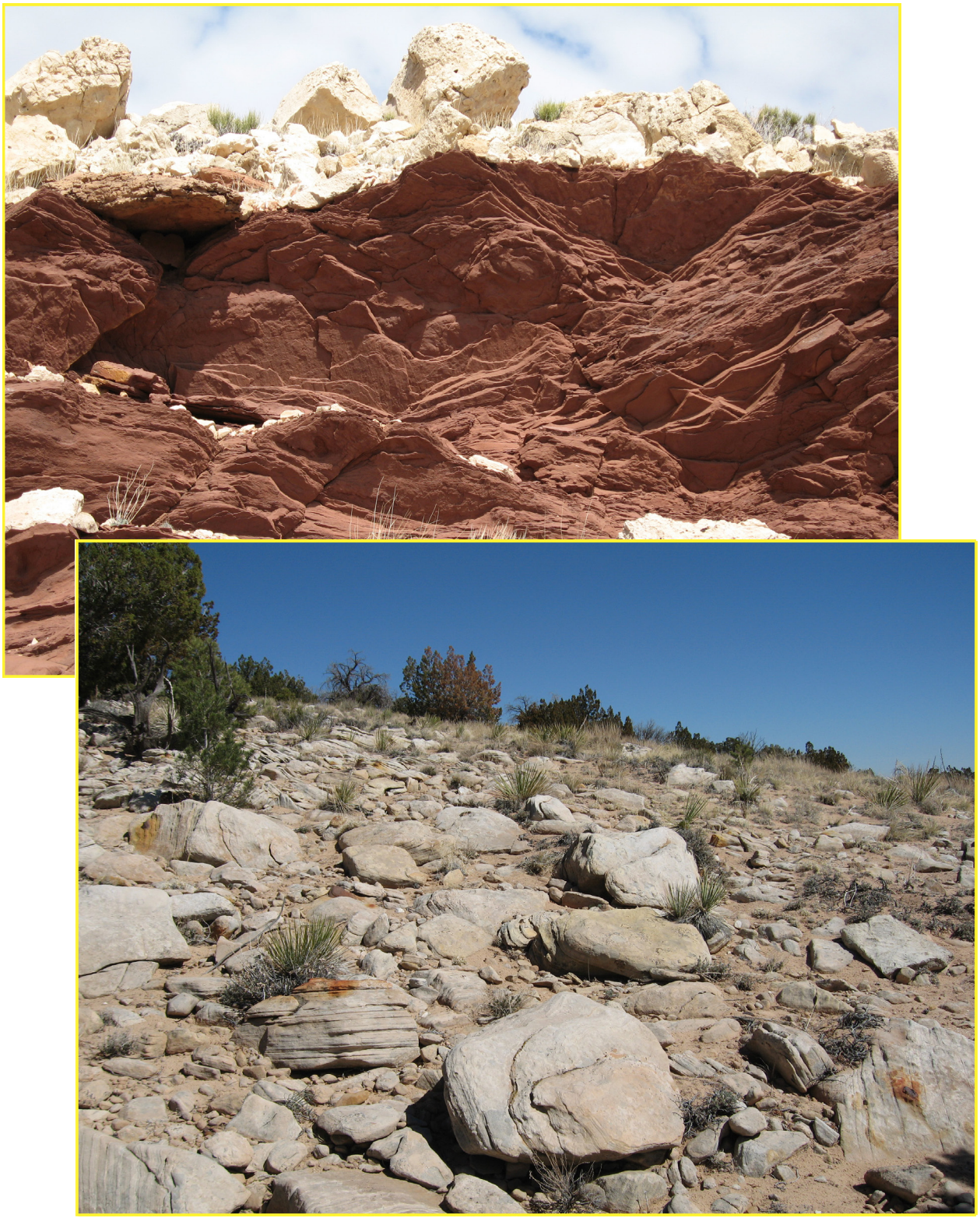

Fig. 8.5. Examples of Moenkopi, Kaibab, and Coconino-Toroweap ejecta in the continuous overturned ejecta blanket. Overturned and ejected Moenkopi is relatively unfractured and forms a coherent unit below a more disrupted layer of Kaibab debris (top panel). This view is along the north wall of the crater. Overturned Coconino-Toroweap ejecta is disrupted even further (bottom panel), with boulders often limited to diameters of only a few tens of centimeters. This view is on the south side of the crater, beyond the crater rim.

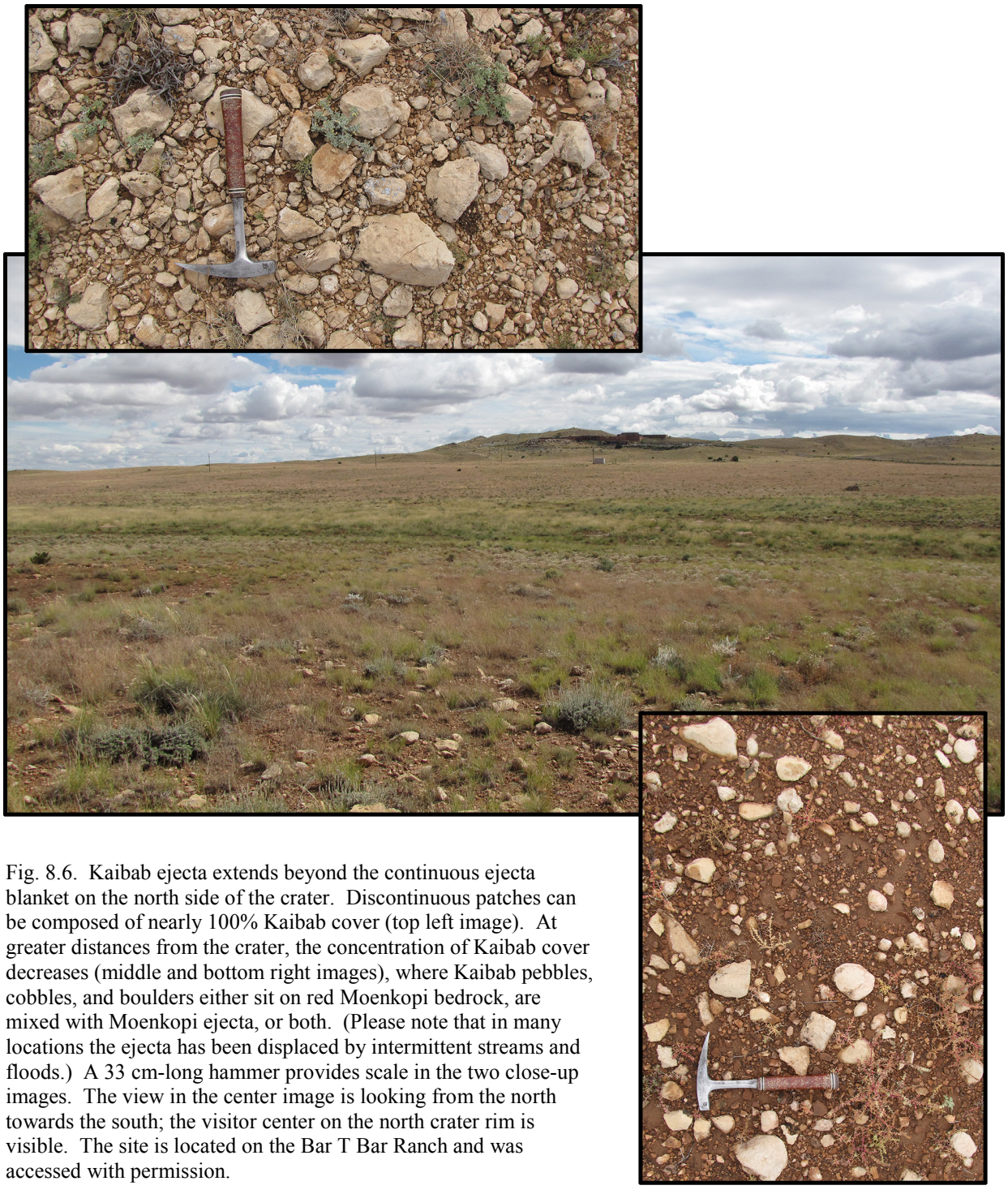

Fig. 8.6. Kaibab ejecta extends beyond the continuous ejecta blanket on the north side of the crater. Discontinuous patches can be composed of nearly 100% Kaibab cover (top left image). At greater distances from the crater, the concentration of Kaibab cover decreases (middle and bottom right images), where Kaibab pebbles, cobbles, and boulders either sit on red Moenkopi bedrock, are mixed with Moenkopi ejecta, or both. (Please note that in many locations the ejecta has been displaced by intermittent streams and floods.) A 33 cm-long hammer provides scale in the two close-up images. The view in the center image is looking from the north towards the south; the visitor center on the north crater rim is visible. The site is located on the Bar T Bar Ranch and was accessed with permission.

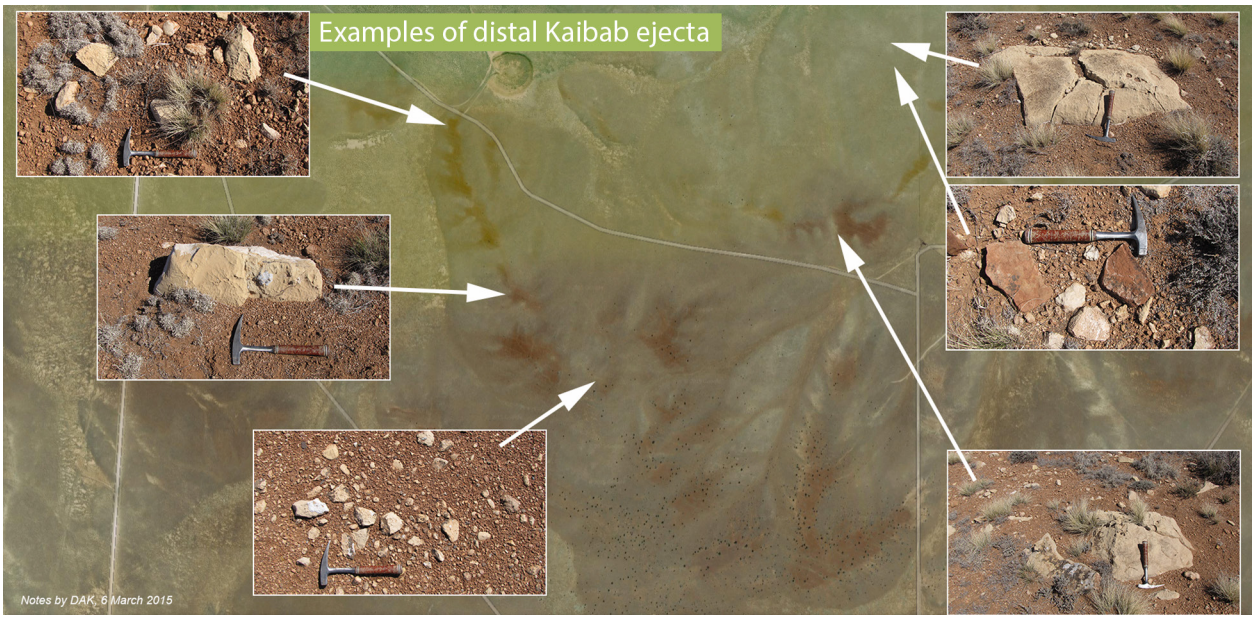

Fig. 8.7. Beyond the continuous ejecta blanket are scattered pebbles, cobbles, and boulders of Kaibab ejecta sitting on a surface of Moenkopi. The atlas of examples shown here are on the south side of the crater on the Bar T Bar Ranch and studied with permission. The example in the upper left is composed of all three particle sizes. Caliche rinds partially surround many specimens, indicating previous burial and exhumation. That is, the ejecta unit used to be thicker than it now appears. The boulder in the second panel (moving counter-clockwise) is on a ridge with vegetation lines, indicating Moenkopi bedrock. In some cases, the Kaibab could be mixed with Moenkopi ejecta too, but that is difficult to discern when sitting on top of a degraded Moenkopi surface. Some of the debris near the boulder in the lower right panel has solution pits (forming tear pants texture), indicating significant subaerial exposure to acidic rain. The most distant example pictured (bottom center) is 2¼ km from the crater center. The circular feature in the top center of the frame is a cattle tank. The crater is located farther north, beyond the field of view.

Fig. 8.8. (top panel) Kaibab ejecta on a ~6 m-high Moenkopi ridge ~1.2 km beyond the crater rim. The lobe of material is outlined with a dashed line. The crater is to the left of the image, so the material was flowing radially to the right after landing. (bottom panel) Discontinuous ejecta can be nearly 100% Kaibab (as seen here), although it also contains cobbles of the Kaibab-Moenkopi boundary breccia and pebbles of Moenkopi (as seen outside the frame of this image). This material was initially mapped as alluvium by Shoemaker. Grant and Schultz (1993; see their Fig. 12) subsequently suggested it was ejecta and, I might add, convinced David Roddy who introduced the deposit to me about twenty years ago. See Kring *et al.* (2015) for additional details about the deposit. Note: This outcrop, like all those around the crater, can only be visited with permission. Also, because this material, like nearly all impact-generated material around the crater, is unconsolidated, please do not step on it or otherwise disturb the geologic evidence of the processes that produced the deposit.

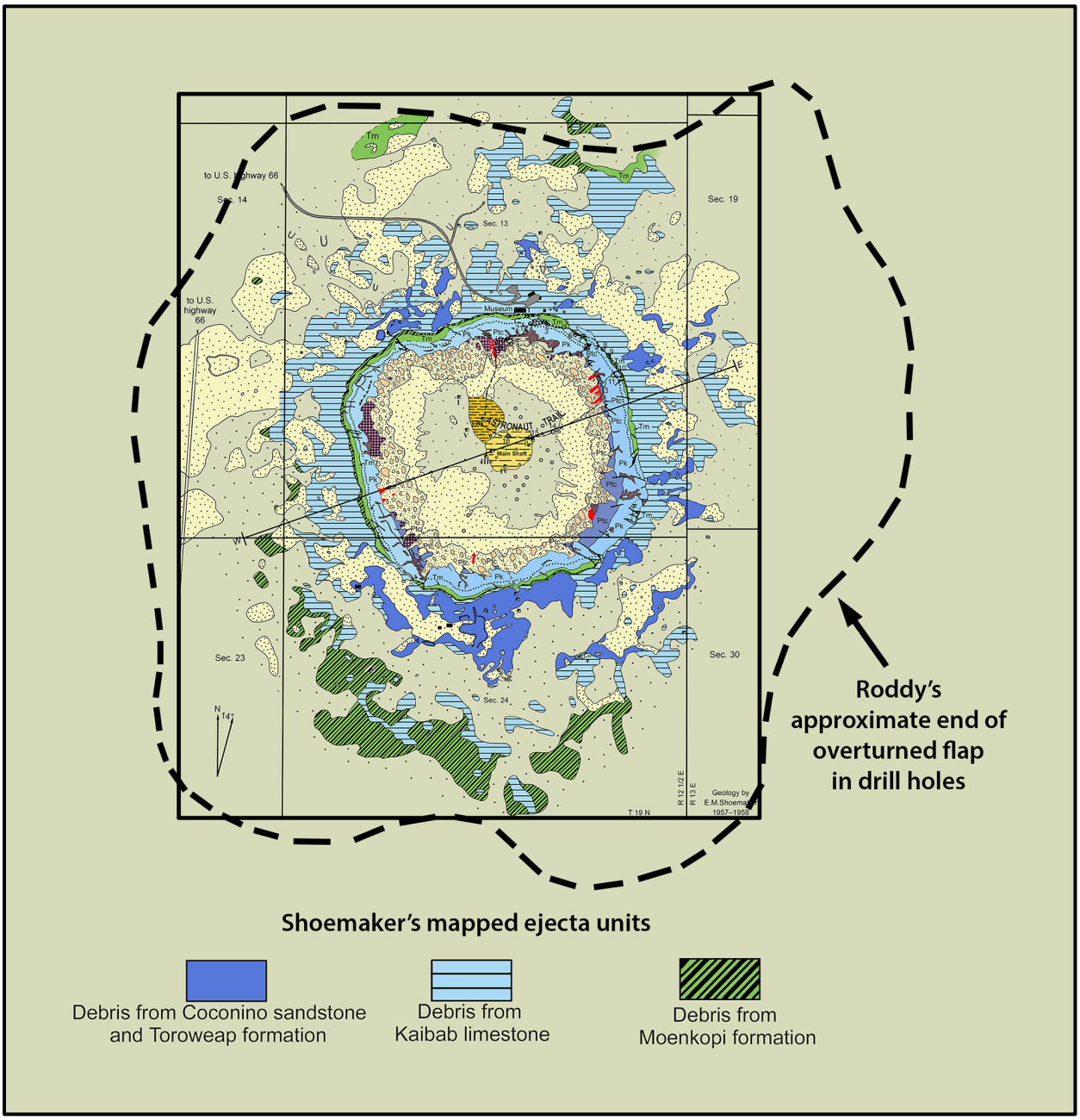

Fig. 8.9. Shoemaker mapped (1957-1958) the impact ejecta units visible in the surface, which provides a minimum estimate of the radial extent of the continuous ejecta blanket. Roddy *et al.* (1975) led a drilling campaign that probed the subsurface, including those areas that are currently covered with alluvium. Based on the cuttings produced by that drilling, he estimated the extent of the overturned flap (*i.e.*, the continuous ejecta blanket) to be significantly larger than that discernable in the surface geology.

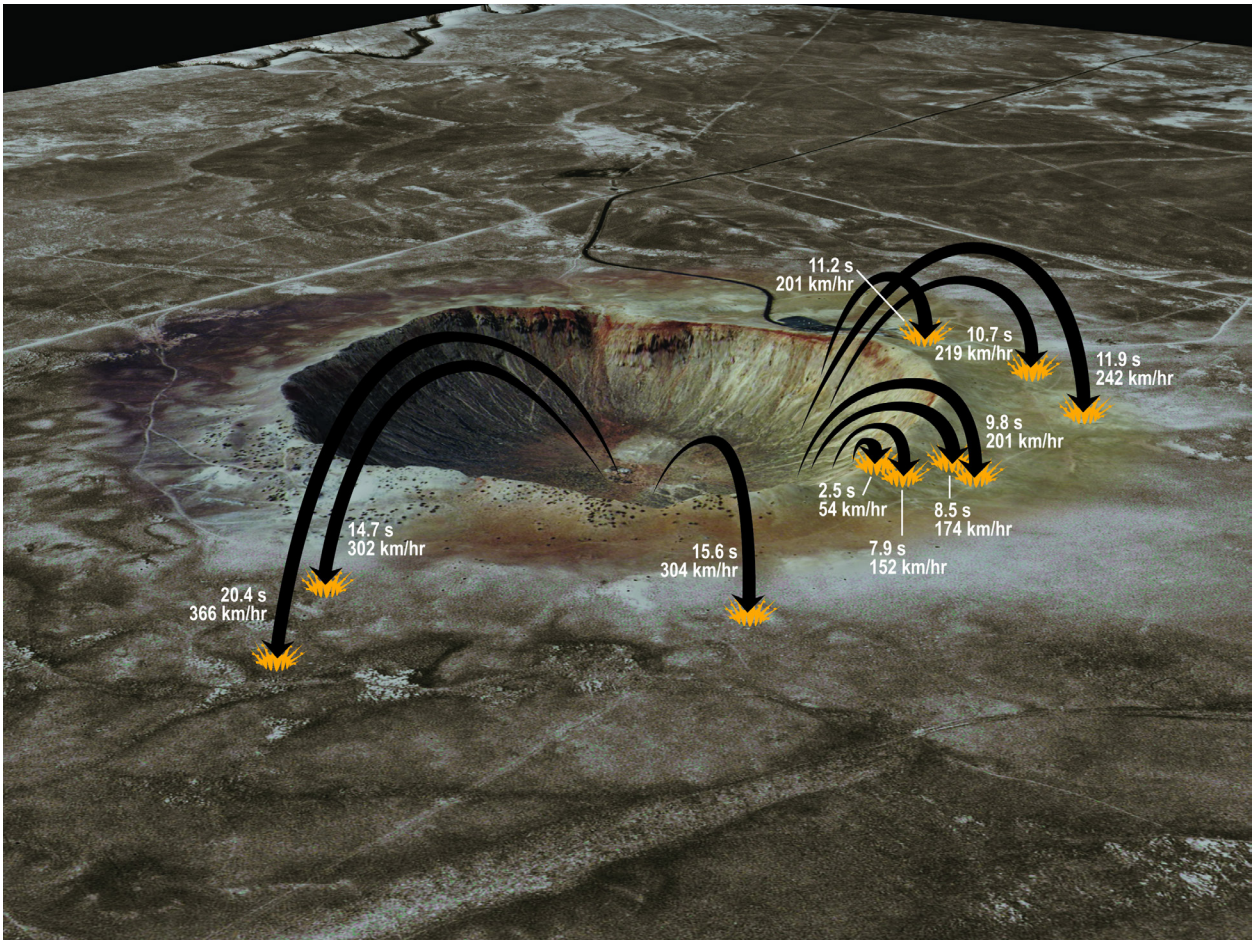

Fig. 8.10. Components in the ejecta curtain are traveling on ballistic trajectories. The debris at the base of the overturned ejecta flap landed first at modest speeds, while more distal portions of the continuous ejecta blanket landed later in time and at higher speeds. For example, one of the largest blocks visible near the crater rim is called Monument Rock or House Rock. It landed about 2 seconds after being launched and hit with a speed of about 50 km/hr. In contrast, a block landing about half a kilometer beyond the crater rim hit with a speed of about 370 km/hr.

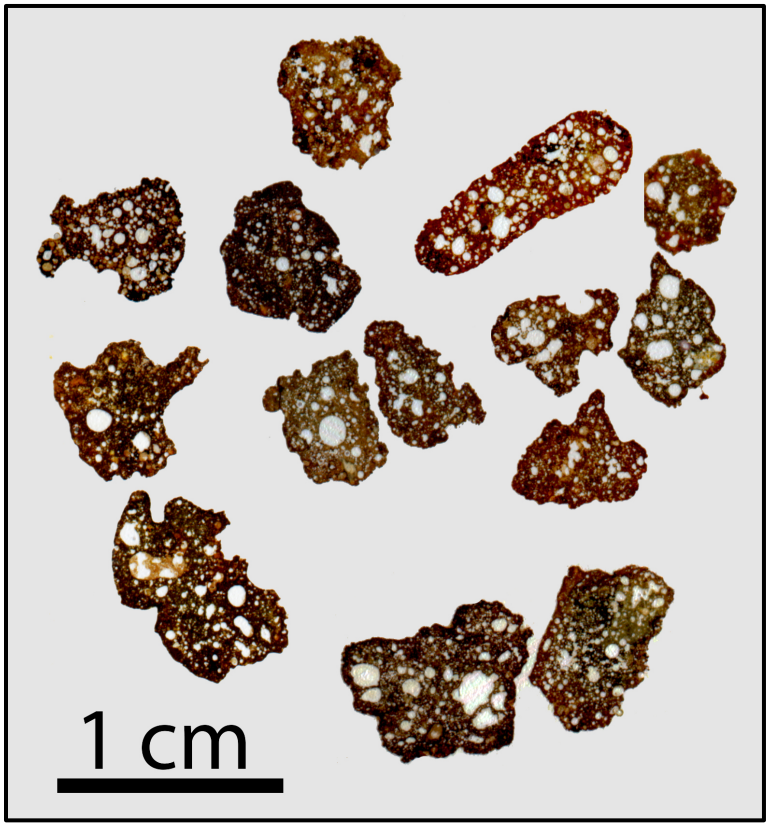

Fig. 8.11. An array of small impact melt particles that were recovered from the eroded surface of the ejecta blanket. The particles are glassy, vesicular, and contain olivine and pyroxene that grew before the melts were completely quenched. The melts are mixtures of degassed target rocks, dominantly the sandy dolomite of the Kaibab, and siderophile elements from the iron asteroid.

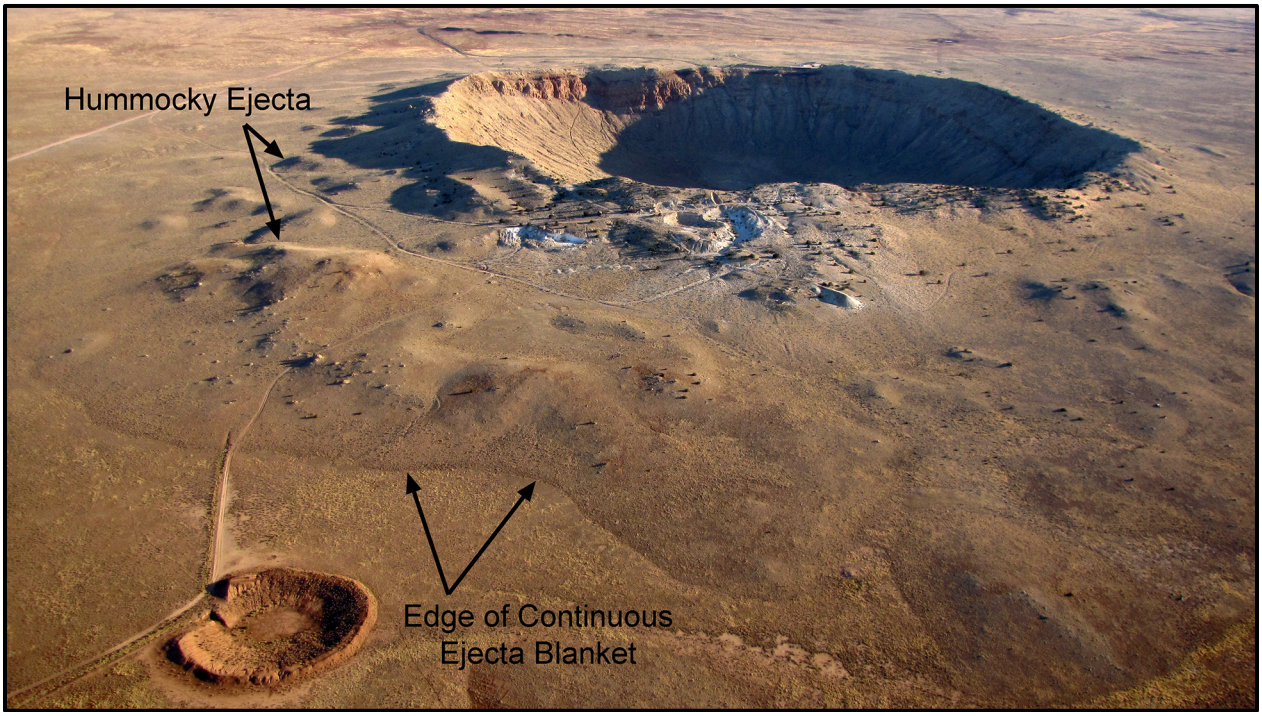

Fig. 8.12. The continuous ejecta blanket around Meteor Crater has a hummocky topography, as illuminated at dawn when the sun angle is very low. Also visible is the edge of the ejecta blanket, which corresponds to the ejecta mapped by Shoemaker (1960), although Roddy *et al.* (1975) argued the ejecta blanket extends farther and lies beneath Quaternary cover. The view is from the south to the north.